STEAM RECEIVER MODELS FOR SOLAR DISH CONCENTRATORS: TWO MODELS COMPARED

José Zapata, Keith Lovegrove and John Pye

Solar Thermal Group, Australian National University (ANU)

Department of Engineering, Building 32 North Rd, ACT 0200, Australia. Ph+61 2 6125 3072

jose.zapata@anu.edu.au

1. Abstract

This paper presents two approaches developed at the Australian National University for modelling the transient response of a parabolic dish steam cavity receiver. Both approaches are based on a heat transfer model for a cylindrical pipe using a moving-boundary formulation, and feature the ability to model multiple phase flow that changes dynamically. A model simulation is implemented in TRNSYS 16 and compared against an experimental run for the ANU 500m² "SG4" system.

2. Introduction

Whilst much work internationally on dish concentrator systems has looked at their application with Stirling engines, they are also well suited to the operation of direct steam generating receivers that can produce the highest temperatures and pressures that commercial steam turbines operate at. It is envisaged that plants based on large arrays of dishes would operate by collecting the steam from all the dishes and transporting it to a central power block via a steam line network.

Transient modelling for a solar thermal energy plant is crucial for the accurate estimation of its performance. Furthermore, an accurate model can provide insights into the plant's design and possibilities for optimisation. Another feature of a transient model is its usefulness in developing an automatic control system.

This paper reviews the transient model of a dish steam cavity receiver developed by Siangsukone [1] and compares it with a new model currently under development at the ANU Solar Thermal Group. Both models are described and compared. A qualitative analysis is also included discussing the relative merits of each approach. Experimental results of the new dish are compared with a simulation, which is part of ongoing work by the authors.

3. Dish Systems at ANU

The ANU has pioneered the design of very large dish concentrators. Figure 1 shows the 400m2 "SG3" system completed on the campus in 1994 and the 500m2 "SG4" system completed in mid 2009. [2]

Figure 1: The 400m^2 "SG3" system (left) and the new 500m^2 "SG4" system (right) during experimental runs

The SG4 dish is currently being operated with the monotube boiler direct steam generation receiver that was previously used on the SG3 dish. The higher concentration ratio of the new dish has allowed the same receiver to be used even though the SG4 dish is larger.

The steam cavity receiver consists of a winding of steel tube coiled around a conical or taper section and cylindrical section to form a cavity (see Figure 2). The feed water enters the receiver at the beginning of the conical section and exits at the end of the top section. The steel tube is comprised of approximately 110m of 16mm OD pipe and 95m of ¾ inch pipe.

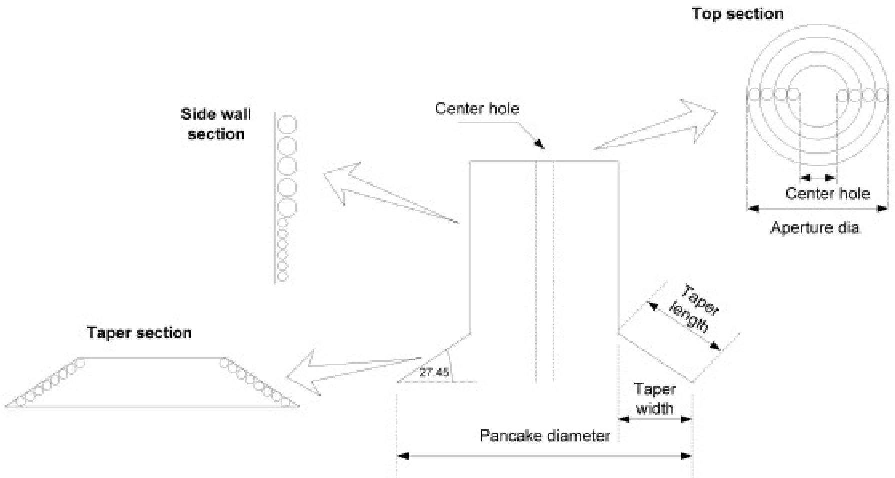

Figure 2: Steam Cavity Receiver design used in SG3 and SG4 dish systems

The exterior of the cavity is covered with 200mm thickness mineral wool insulation and enclosed with sheet metal.

This receiver has been successfully fitted to the SG4 receiver and carried out a preliminary test on the 6th of August 2010. In this test the outer tapered section, which is intended to capture the outer low concentration parts of the focal region distribution, was covered with a ceramic blanket. Feed water was pumped to the receiver, and steam was allowed to vent off to atmosphere, while it was tracking the sun. Table 1, summarises the operating conditions obtained at steady state for three mass flow settings.

Mass Flow [g/s]	Outlet Temp [°C]	Outlet Steam Power [kW]	Receiver Thermal Efficiency [%]
97	502	333	85
120	283	357	92
129	177	362	94

Table 1: Summary of Experimental run carried out on the 6th of August 2010

The overall thermal efficiency is defined as the ratio of the change in thermal energy of the fluid and the dish solar radiation captured by the receiver. The calculation is expressed in equation (1), where A_{dish} is the dish mirror area, I_N is the incident normal radiation at the time of the experiment, r is the average reflectivity of the mirrors in the dish and f is a factor of interception, as calculated in [2]The measured reflectivity was 0.91, direct beam radiation was measured at 920W/m² and the operable mirror area was 489m².

$$\eta_t = \frac{\dot{m}_i (h_o - h_i)}{A_{dish} I_N r f} \quad (1)$$

4. Description of Models

There are two main approaches currently used to model the transient behaviour of boilers; the finite element method and the moving-boundary model method[3,4]. The moving-boundary method is seen as a middle ground between a lumped parameter model and a finite element model, with the advantage of being more accurate than a lumped parameter model and less computationally expensive than a finite element model. Both models in this paper follow the moving-boundary approach where a series of time-varying sized regions contain the different phases of water as it traverses through the boiler.

4.1. Siangsukone Model

A detailed transient model and simulation of the Australian National University's 400m^2 Solar Generation 3(SG3) system was developed by Piya Louis Siangsukone [1]. This model is derived from first principles for the steam cavity receiver of the SG3 system and validated by comparing experimental data with TRNSYS simulations.

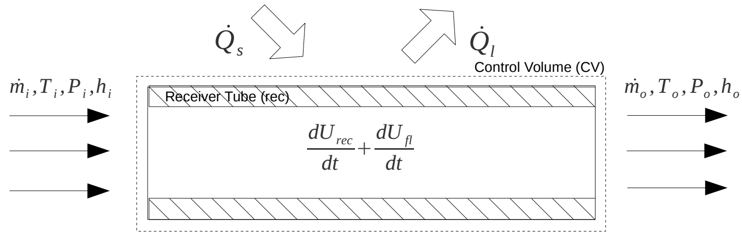

Figure 3: Control Volume for Cavity Receiver (adapted from [1])

It can handle sub-cooled water, saturated mixture and superheated steam coexisting in the evaporator and the dynamic disappearance/appearance of any of the regions. It also incorporates a linear pressure drop correlation to compensate for the extended length of the cavity receiver pipe. The properties of the fluid are averaged within all regions. For the single phase regions a temperature gradient is derived to predict the dynamic behaviour of sub cooled water and super heated vapour. For the two phase region a specific volume gradient is derived to estimate the dynamic behaviour of the saturated water/steam mixture.

This model is implemented in the TRNSYS simulation environment and it is possible to create multiple instances connected in series to allow greater spatial resolution of conditions such as incident flux.

4.2. Model Derivation

A simplified energy balance equation of a straight cylindrical pipe carrying a moving heat transfer fluid and subjected to an incident heat flux (Figure 3) can be derived:

$$\dot{Q}_s - \dot{Q}_l + \dot{m}_i h_i - \dot{m}_o h_o = m_{rec}\frac{du_{rec}}{dt} + m_{fl}\frac{du_{fl}}{dt} + u_{fl}\frac{dm_{fl}}{dt} \quad (2)$$

Where $\dot{Q}_s$ is the incident solar flux and $\dot{Q}_l$ are the radiation and convection losses from the receiver and the subscripts *rec* and *fl* pertain to the receiver and fluid respectively. Radiation and convection losses can be derived from:

$$\dot{Q}_l = G\epsilon A_{tube}(T_{cv}^4 - T_a^4) + UA_{tube}(T_{cv} - T_a) \quad (3)$$

Heat losses are modelled using a geometrical correlation factor G for the radiative portion and a heat transfer factor U for the convective portion that have been determined experimentally. In equation (3) the subscript *cv* refers to the combined receiver and fluid control volume, as it is assumed that the receiver tube will be at the same average temperature as the fluid.

Additional assumptions are required to proceed with the derivation of this model: kinetic and potential energy of the fluid do not change traversing through the section of tubing; fluid properties are averaged along sections of tubing where the fluid is of a particular phase (sub-cooled, saturated mixture, super-heated); heat flux is uniformly distributed along the pipe sections. These and other considerations are often seen in models which focus on the transient aspects of heat transfer[3]-[6].

For the single phase regions, it is established that the rate of change of fluid mass is negligible in comparison with the other terms of the energy equation for a single time step, eliminating the need for the third term of the right hand side of equation (2). Additionally, single phase fluids are considered at constant pressure, which means that the internal energy of the tube and fluid only depend on the temperature of the control volume.

$$\frac{du_{rec}}{dt}=c_{rec}\frac{dT_{cv}}{dt}\rightarrow\frac{du_{fl}}{dt}=\frac{du_{fl}}{dT_{cv}}\left[\frac{dT_{cv}}{dt}\right]\approx\frac{\Delta u}{\Delta T}\frac{dT_{cv}}{dt} \tag{4}$$

This implies that the transient energy balance in a single phase region is linked to a rate of change in temperature. It is therefore possible to rewrite the energy balance in terms of a transient temperature change. Substituting (3) into (2) and re arranging for the rate of change of temperature of the fluid and receiver, equation (5) is obtained.

$$\frac{dT_{cv}}{dt}=\frac{\dot{Q}_s-A_{tube}\left[G\epsilon\sigma(T_{cv}^4-T_a^4)+U(T_{cv}-T_a)\right]+\dot{m}_i(h_i-h_o)}{m_{rec}c_{rec}+m_{fl}\frac{\Delta u}{\Delta T}} \tag{5}$$

When the fluid is a mixture of saturated liquid and vapour, the rate of change of internal energy cannot only depend on temperature, as the average specific volume of the mixture changes with the fraction of vapour mass to total mass in the control volume. In addition to this, when the pressure is held constant, the transient temperature change is zero, due to the fluid being saturated.

$$\begin{gathered}\frac{du_{rec}}{dt}=c_{rec}\frac{dT_{cv}}{dt}=0\\ \frac{du_{fl}}{dt}=\frac{du_{fl}}{d\nu}\left[\frac{d\nu}{dt}\right]\approx\frac{\Delta u}{\Delta\nu}\left[\frac{d\nu}{dt}\right]\end{gathered} \tag{6}$$

In equation (6) are expressed the conditions of the mixture region, which together with the energy balance of equation (2) are rearranged into equation (7), which links the change of energy in the two-phase fluid to the rate of change of its specific volume.

$$\frac{d\nu}{dt}=\frac{\dot{Q}_s-A_{tube}\left[G\epsilon\sigma(T_{cv}^4-T_a^4)+U(T_{cv}-T_a)\right]+\dot{m}_i(h_i-h_o)}{m_{fl}\frac{\Delta u}{\Delta\nu}+(h_o-u_{fl})\frac{V_{fl}}{\nu^2}} \tag{7}$$

The finite difference method is then use to work out the increase in energy in the fluid.

$$\begin{gathered}T_{cv}(t+\delta t)=T_{cv}(t)+\delta t\cdot\frac{dT_{cv}}{dt}\\ \nu(t+\delta t)=\nu(t)+\delta t\cdot\frac{d\nu}{dt}\end{gathered} \tag{8}$$

Where δt is the simulation time step.

4.3. Calculation of energy changes and phase changes

In order to establish which expression should be used to calculate transient energy change inside the receiver, the inlet conditions of the fluid have to be examined. If the incoming fluid is sub-cooled liquid or super-heated steam, then expression (5) is used. If the inlet fluid conditions are of a saturated mixture, then (6) is used. During normal operation, the feed water passing through the cavity receiver will transition from single phase liquid, to saturated mixture and into super-heated steam. It is thus necessary to establish when these transitions occur to accurately apply a transient change of temperature or specific volume when applicable.

The outlet temperature is calculated from the inlet fluid temperature and the average control volume temperature:

$$T_o=2\mathrm{T}_{cv}-T_i \tag{9}$$

If the outlet temperature is greater or equal to the saturation temperature of the fluid at the control volume pressure, then a liquid region length is calculated. This means that before exiting the tube, the fluid changes phase and equation (7) has to be used to calculate the change in energy for the reminder of the tube. The fluid conditions at the exit of the liquid region, i.e. mass flow, temperature and pressure are the conditions at the inlet of the mixture region. It is important to note that the heat flux and receiver tube mass quantities in the transient equations (5) and (7) are linked to these calculated region lengths.

Subsequently, if the outlet specific volume of the mixture region is equal or greater than the specific volume of saturated vapour, then a liquid mixture region length is determined, and a temperature rate of change using (5) is calculated for the super-heated steam. The length of the super-heated region is the length of the tube minus the combined length of the liquid and saturated regions.

4.4. Pressure Drops in the control volume

It has been mentioned that for each region, the pressure of the fluid is assumed constant and furthermore equal to the pressure at the inlet of such region. It is however needed to account for pressure drops in the cavity receiver due to the length of the tube. A static correlation (Darcy-Weisbach[7] correlation) is applied with a factor *K* to fit the model with measured experimental data.

$$\Delta P = K\left[f L_{region} \frac{\rho U_m^2}{4r} \right] \tag{10}$$

The friction factor *f* is calculated from the formulation of Swamee and Jain[8]. Therefore the pressure at the outlet of each region will be the pressure at the inlet minus this calculated pressure drop. The recalculation of these pressure drops at each time steps allows a more refined determination of the properties of the fluid travelling through the receiver.

4.5. Proposed Model Description

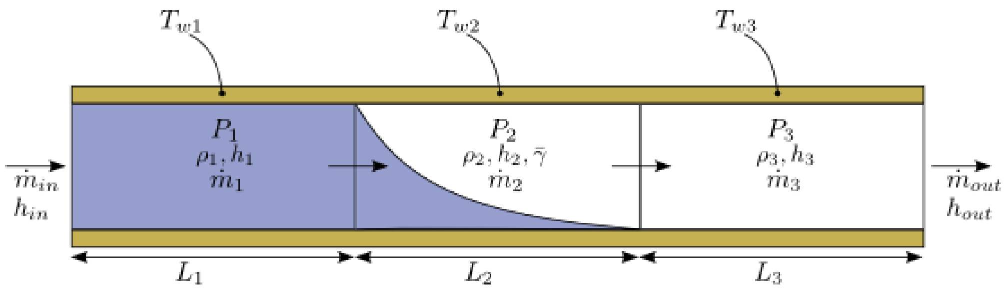

Figure 4: Control Volume for Cavity Receiver in moving-boundary formulation

The present study has been developed with the purpose of producing a model-based predictive control scheme for a dish steam cavity receiver plant. It combines a moving-boundary approach as used by Tummescheit and Jensen[3,4] with a novel equation-switching strategy by McKinley[5] and incorporates a pressure drop calculation by Yebra[6]. One of the aims of this model is to match the benefits of the Siangsukone approach, i.e. dynamically switching the number of regions and accounting for pressure drops in the evaporator. This approach also provides explicit time derivatives of all the variables in the model, which is currently not possible in the existing model, providing greater insight into the dynamic behaviour of the receiver. This structure is also useful for devising control strategies for the operation of the system.

4.6. Derivation of Proposed Model

Figure 4 represents the control volume of the steam cavity receiver. It is subdivided in three regions of sub-cooled water, saturated mixture and super-heated steam. Each region occupies a length in the pipe, L_1, L_2 and L_3 respectively. An unsteady balance of fluid mass, fluid energy, fluid momentum and wall energy is derived for each region forming a system of ordinary differential equations of the form

$$\boldsymbol{Z}\dot{\boldsymbol{x}} = \boldsymbol{f}(\boldsymbol{x}, \boldsymbol{u}, t) \tag{11}$$

Where the state vector $\boldsymbol{x}$ is expressed in (12), the matrix $\boldsymbol{Z}$ contains the equation coefficients and $\boldsymbol{f}$ is the forcing function of the system.

$$\boldsymbol{x}=\left[L_1\ L_2\ P_1\ \dot{m}_1\ P_2\ \dot{m}_2\ P_3\ \dot{m}_3\ h_{out}\ T_{w1}\ T_{w2}\ T_{w3}\ \bar{\gamma}\right] \tag{12}$$

The state vector denotes that there are 13 variables simultaneously calculated in the system, including the lengths of the regions,mass flows, pressures and wall temperatures. The time derivative of all the state variables is explicitly declared in the set of equations, meaning that not only the state of the system is known but also the rate of change of all the states. Note that the void fraction $\bar{\gamma}$ is considered time-varying, and therefore a state of the system. This is incorporated to allow the switching of equations when the control volume changes the number of regions present.

If the number of regions present in the system changes, the number of conservation equations and therefore the coefficients of the matrix $\boldsymbol{Z}$ would change as well. If this was the case, the matrix $\boldsymbol{Z}$ would become singular and the equations unsolvable. To overcome this, pseudo-equations are introduced for each one of the states that are currently not present in the system [5]. For example, if there was not a region of super-heated steam present, the states $P_3, \dot{m}_3, T_{w3}$ would not exist and therefore the following equations would take their place:

$$\frac{dP_3}{dt}=K_P(P_2-P_3)\ \frac{d\dot{m}_3}{dt}=K_m(\dot{m}_2-\dot{m}_3)\ d\frac{T_{W3}}{dt}=K_{T_w}(T_{w2}-T_{w3}) \tag{13}$$

Here it is appreciated that a first order dynamic is introduced so that the non existent states track the values of the existing adjacent states. This enables the variables to have a sensible initial value when the system of equations switches to a form that contains all regions. The time constants are calibrated specifically for the steam cavity receiver, to be orders of magnitude faster than the system time constants, but taking care to avoid stiffening the system solution.

4.7. Switching Criteria

Analogously to Siangsukone's approach, it is desired that the model handles all operation modes of the system. It is therefore required that the system models the appearance/disappearance of each region. There are six possible combinations of regions as shown in Figure 5:

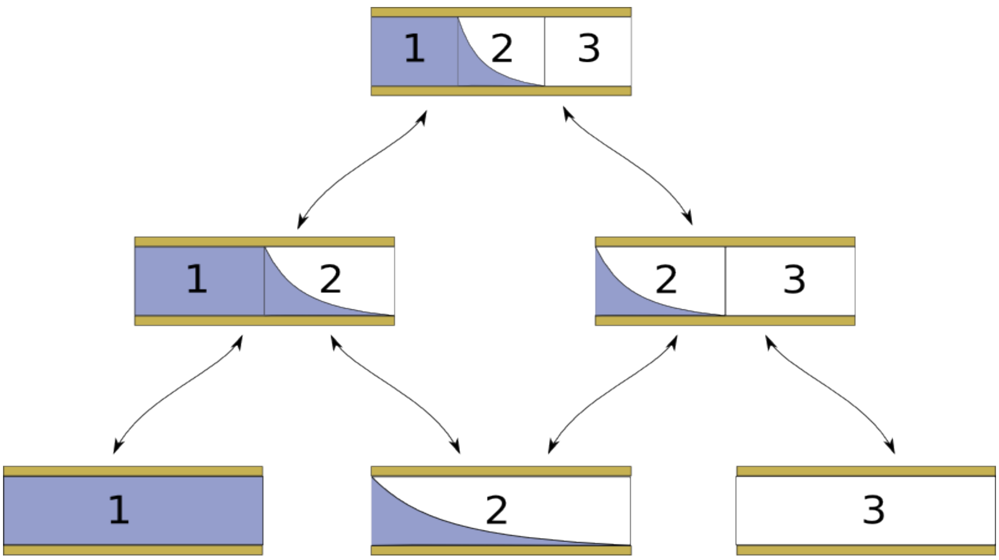

Figure 5: Possible Switching Combinations for Steam Cavity Receiver Model

In this work a set of conservation equations for each case depicted in Figure 5 has been developed. Furthermore, the diagram shows that only certain transitions are allowed between states, and these are consistent with a progressive heating or cooling of the steam cavity receiver. The cases where no sub-cooled region is present are required when multiple instances of the model are connected in series in a simulation, for the purpose of better capturing the incoming flux hitting the receiver. The appendix contains expressions for the matrix $\boldsymbol{Z}$ and vector $\boldsymbol{f}$ for the case of regions types 1,2 and 3,as labelled in the figure, existing simultaneously.

In order to transition from one set of equations to the next, the outlet or inlet conditions of the control volume have to be examined. For example, consider a receiver which is currently being heated by an incident heat flux, and contains regions of types 1 and 2. If the fluid continues to heat, eventually a super-heated region will appear. Therefore it is of interest to know if there exists complete evaporation in the saturated region. Since the specific enthalpy of the fluid depends on the void fraction $\bar{\gamma}$, it is examined against the void fraction at full evaporation:

$$L_2(\bar{\gamma}_{tot}-\bar{\gamma})<L_{min} \text{ and } \frac{d\bar{\gamma}}{dt}>0 \tag{14}$$

In expression (14) L_{min} is an arbitrarily small value and the void fraction is multiplied by L_2 in order to ensure the comparison is performed at a representatively sized saturated region. If the void fraction of the saturated region is arbitrarily close to the void fraction at complete evaporation, and continues to increase, then the system is switched to a 3 region boiler.

5. Model Comparison

There are many similarities between Siangsukone's model and the proposed model, mainly due to the fact that the proposed model has to, at least, match all the features of Siangsukone's model. These include: A transient response heat transfer with multiple phase flow, incorporation of radiative and convective losses in the receiver, pressure drop correlations and the ability to connect multiple instances of the model in series to better capture the incoming flux distribution.

It is desired that the proposed model is an improvement on Siangsukone's model for the following reasons: thanks to being expressed as a set of differential equations, control theory can be applied on the model to derive optimum mass flow profiles. The proposed model is more detailed in calculating the fluid properties and heat transfer mechanisms, for instance, Siangsukone's model assumes the pipe wall and the fluid have the same temperature.There is more versatility in the model calibration as many parameters are considered for each region (e.g. heat transfer coefficients) as opposed to system wide. This however means that there is a potential for more complexity in the calibration of the simulation, when validating with experimental runs.

6. Simulation of the Cavity Receiver in TRNSYS

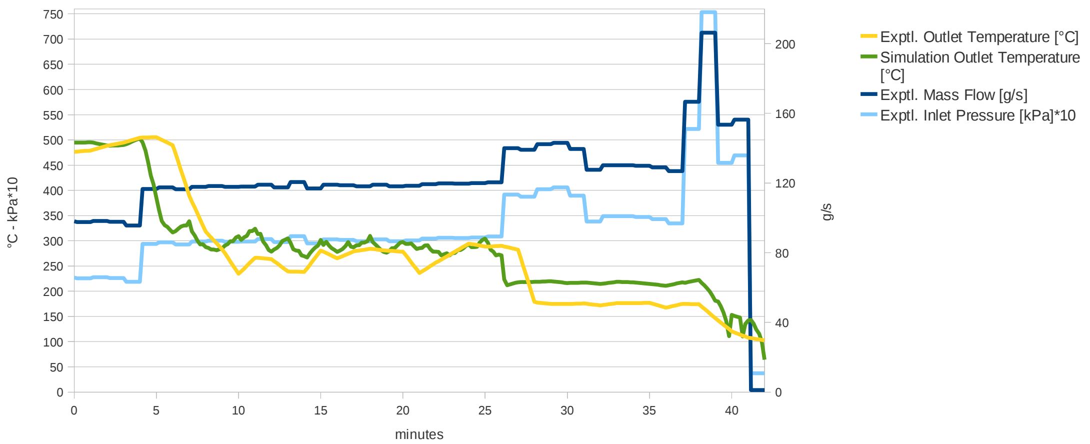

Figure 6: Comparison of experimental data and TRNSYS simulation using Siangsukone's model

A simulation of the SG4 system during the experimental run on the 6th of August 2010, using Siangsukone's model in TRNSYS 16 is presented in Figure 6. The simulation takes the measured feed water mass flow, insolation, ambient temperature and other measurements to calculate the transient response of the receiver. In the experimental run, mass flow rates are maintained until the fluid temperature of the receiver reaches steady state.

In this experiment, the steam is blown off to ambient after passing through the receiver, which affects pressure drop over the receiver length, in comparison to a receiver connected to a steam generation system. The graphs show that the mass flow and inlet pressure are closely related. The feed water mass flow exhibits small variations around each set point, which are also reflected and amplified in the inlet pressure. This creates a complex pressure drop profile in the receiver. The simulation assumes less drastic changes and variations in pressure and this may cause the fluid properties, and temperatures to be estimated incorrectly.

There is also a time delay in the simulated temperature in response to changes in mass flow. This indicates that the time constants of the system may not have been accurately reproduced in the simulation, or that there is a time lag in the response due to other reasons.

It is apparent that the experimental results indicate a system with a much longer time constant than the modelled results. Siangsukone's model achieved good agreement between TRNSYS simulations and the SG3 dish using the same receiver, after careful calibration of the system parameters. Those experiments were carried out with steam fed to a reciprocating steam engine that maintained back-pressures up to 4MPa. It is suspected that the low pressure exit conditions are the reason for the lack of agreement for this first test.

The authors have yet to find good agreement between experimental data and model simulations, but this effort is part of an ongoing work and several aspects of this discrepancy are the current focus of their research.

7. Conclusion

Two modelling techniques for the transient simulation dish based steam cavity receiver at the ANU have been presented. The main features of each of the techniques have been discussed. The second model is currently under development and it is intended to be an improvement on Siangsukone's model, for the purpose of system simulations, optimisation and control. The Siangsukone model has previously been successfully applied to predicting the behaviour of a monotube boiler receiver on the ANU 400m^2 dish.

The first experimental run of the 500m^2 SG4 system with the same monotube steam system sho receiver efficiencies of 84% at 500°C and up to 94% at lower temperatures. This is encouraging performance particularly given that the operating configuration is not yet optimised. Initial modelling with the Siangsukone model using the same parameters as used for the 400m^2 dish do not yet show good agreement.

Work continues on experimental investigations and calibration of the two models to the new system reproducing the transient behaviour of the dish in a transient simulation environment.

Acknowledgements

The authors wish to thank the assistance of the Solar Thermal Group at the Australian National University in the preparation of this paper, specifically with regards to the experimental runs: Mr Greg Burgess, Mr Wie Joe and Mr Geoff Major.

References

[1] Piya Louis Siangsukone. *Transient Simulation and Modeling of a Dish Cavity Receiver*. PhD thesis, Australian National University, September 2005.

[2] K. Lovegrove, G. Burgess and J. Pye, A new 500m^2 parabolidal dish solar concentrator, *Solar Energy*, In Press.

[3] J.M. Jensen and H. Tummescheit. Moving boundary models for dynamic simulations of two-phase flows. In *Proc. of the 2nd Int. Modelica Conference*,2002.

[4] Hubertus Tummescheit. *Design and Implementation of Object-Oriented Model Libraries using Modelica*. PhD thesis, Department of Automatic Control, Lund Institute of Technology, August 2002.

[5] T.L. McKinley and A.G. Alleyne. A switched system model for heat exchangers using a moving boundary method. In *Proc. American Control Conference*, pages 1455–1462, 2008.

[6] L.J Yebra, M. Berenguel, and S. Dormido. Extended moving-boundary models for two-phase flows. In *Proceedings of the IFAC 2005*, 2005.

[7] Potter M.C. And Wiggert D.C. *Mechanics of Fluids*, Prentice-Hall, Inc. New Jersey, USA. 1991.

[8] Swamee P.K., and Jain A.K. Explicit Equations for Pipe Flow Problems.*Journal of the Hydraulics Division*,Vol. 102, No. 5, May 1976, pp. 657-664

Appendix: Coefficients of Matrix *Z* for boiler

$$
\boldsymbol{f}=\begin{bmatrix}
\dot m_i-\frac{1}{2}(\dot m_1+\dot m_2)-\frac{1}{2A}L_1\frac{\partial\rho_1}{\partial h}\frac{dh_i}{dt}\\
\frac{1}{2}(\dot m_1-\dot m_3)\\
\frac{1}{2}(\dot m_2+\dot m_3)-\dot m_o\\
\dot m_i h_i-\frac{1}{2}(\dot m_1+\dot m_2)h_f+k_1 piD_iL_1(T_{w1}-T_1)-\frac{1}{2}AL_1\left(\rho_1+\frac{1}{2}\frac{\partial\rho_1}{\partial h}(h_i+h_f)\right)\frac{dh_i}{dt}\\
\frac{1}{2}(\dot m_1+\dot m_2)h_f-\frac{1}{2}(\dot m_2+\dot m_3)h_g+k_2 piD_iL_2(T_{w2}-T_2)\\
\frac{1}{2}(\dot m_2+\dot m_3)h_f-\dot m_o h_o+k_3 piD_iL_3(T_{w3}-T_3)\\
\frac{\dot m_i|\dot m_i|}{A\rho_i}-\frac{(\dot m_1+\dot m_2)|\dot m_1+\dot m_2|}{4A\rho_f}-\xi L_1\frac{\dot m_1|\dot m_1|}{2A\rho_1 D_i}-A(\frac{1}{2}(P_1+P_2)-P_i)\\
\frac{(\dot m_1+\dot m_2)|\dot m_1+\dot m_2|}{4A\rho_f}-\frac{(\dot m_2+\dot m_3)|\dot m_2+\dot m_3|}{4A\rho_g}-\xi L_2\frac{\dot m_2|\dot m_2|}{2A\rho_2 D_i}-\frac{1}{2}A(P_1+P_3)\\
\frac{(\dot m_2+\dot m_3)|\dot m_2+\dot m_3|}{4A\rho_g}-\frac{(\dot m_o)|\dot m_o|}{A\rho_o}-\xi L_3\frac{\dot m_3|\dot m_3|}{2A\rho_3 D_i}-A(P_o-\frac{1}{2}(P_2+P_3))\\
L_1\left(\dot Q_s-\epsilon\sigma\pi D_o(T_{w1}^4-T_a^4)-h\pi D_o(T_{w1}-Ta)-k\,piD_i(T_1-T_{w1})\right)\\
L_2\left(\dot Q_s-\epsilon\sigma\pi D_o(T_{w2}^4-T_a^4)-h\pi D_o(T_{w2}-Ta)-k\,piD_i(T_2-T_{w2})\right)\\
L_3\left(\dot Q_s-\epsilon\sigma\pi D_o(T_{w3}^4-T_a^4)-h\pi D_o(T_{w3}-Ta)-k\,piD_i(T_3-T_{w3})\right)\\
-K_y(\bar\gamma-\bar\gamma_{tot})
\end{bmatrix}
$$

$$
\boldsymbol{Z}=\begin{bmatrix}
A(\rho_1-\rho_f) & 0 & AL_1\left(\frac{\partial\rho_1}{\partial P}+\frac{1}{2}\frac{\partial\rho_1}{\partial h}\frac{dh_f}{dP}\right) & 0 & 0 & 0 & 0 & 0 & 0 & 0 & 0 & 0 & 0\\
A(\rho_f-\rho_g) & A(1-\bar\gamma)(\rho_f-\rho_g) & 0 & 0 & AL_2\left(\bar\gamma\frac{\partial\rho_g}{\partial P}+(1-\bar\gamma)\frac{\partial\rho_f}{\partial P}\right) & 0 & 0 & 0 & 0 & 0 & 0 & 0 & AL_2(\rho_g-\rho_f)\\
A(\rho_g-\rho_3) & A(\rho_g-\rho_3) & 0 & 0 & 0 & 0 & AL_3\left(\frac{\partial\rho_3}{\partial P}+\frac{1}{2}\frac{\partial\rho_3}{\partial h}\frac{dh_g}{dP}\right) & 0 & \frac{1}{2}AL_3\frac{\partial\rho_3}{\partial h} & 0 & 0 & 0 & 0\\
\frac{1}{2}A(\rho_1(h_i+h_f)-2\rho_f h_f-2P_1+2P(L_1)) & 0 & \frac{1}{2}AL_1\left(\rho_1\frac{dh_f}{dP}+(h_i+h_f)\left(\frac{\partial\rho_1}{\partial P}+\frac{1}{2}\frac{\partial\rho_1}{\partial h}\frac{dh_f}{dP}\right)-2\right) & 0 & 0 & 0 & 0 & 0 & 0 & 0 & 0 & 0 & 0\\
A(\rho_f h_f-\rho_g h_g-P(L_1)+P(L_1+L_2)) & A(1-\bar\gamma)(\rho_f h_f-\rho_g h_g-P_2+P(L_1+L_2)) & 0 & 0 & AL_2\left(\bar\gamma\frac{d(\rho_g h_g)}{dP}+(1-\bar\gamma)\frac{d(\rho_f h_f)}{dP}-1\right) & 0 & 0 & 0 & 0 & 0 & 0 & 0 & AL_2(\rho_g h_g-\rho_f h_f)\\
A(\rho_g h_g-\frac{1}{2}\rho_3(h_g+h_o)+P_3-P(L_1+L_2)) & A(\rho_g h_g-\frac{1}{2}\rho_3(h_g+h_o)+P_3-P(L_1+L_2)) & 0 & 0 & 0 & 0 & AL_3\left(\rho_3\frac{dh_g}{dP}+(h_g+h_o)\left(\frac{\partial\rho_3}{\partial P}+\frac{1}{2}\frac{\partial\rho_3}{\partial h}\frac{dh_g}{dP}\right)-1\right) & 0 & 0 & 0 & 0 & 0 & 0\\
\frac{1}{2}(\dot m_1-\dot m_2) & 0 & 0 & L_1 & 0 & 0 & 0 & 0 & 0 & 0 & 0 & 0 & 0\\
\frac{1}{2}(\dot m_1-\dot m_2) & \frac{1}{2}(\dot m_1-\dot m_3) & 0 & 0 & 0 & L_2 & 0 & 0 & 0 & 0 & 0 & 0 & 0\\
\frac{1}{2}(\dot m_2-\dot m_3) & \frac{1}{2}(\dot m_2-\dot m_3) & 0 & 0 & 0 & 0 & 0 & L_3 & 0 & 0 & 0 & 0 & 0\\
C_w\rho_w A(T_{w1}-T_w(L_1)) & 0 & 0 & 0 & 0 & 0 & 0 & 0 & 0 & C_w\rho_w AL_1 & 0 & 0 & 0\\
C_w\rho_w A(T_w(L_1)-T_w(L_1+L_1)) & C_w\rho_w A(T_{w2}-T_w(L_1+L_1)) & 0 & 0 & 0 & 0 & 0 & 0 & 0 & 0 & C_w\rho_w AL_2 & 0 & 0\\
C_w\rho_w A(T_w(L_1+L_1)-T_{w3}) & C_w\rho_w A(T_w(L_1+L_1)-T_{w3}) & 0 & 0 & 0 & 0 & 0 & 0 & 0 & 0 & 0 & C_w\rho_w AL_3 & 0\\
0 & 0 & 0 & 0 & \frac{-\partial\bar\gamma_{tot}}{\partial P}\frac{dP_2}{dt} & 0 & 0 & 0 & 0 & 0 & 0 & 0 & 1
\end{bmatrix}
$$